Conceptual Design of the Cooling System for a 3D Oil-Immersed Distribution Transformer

Nathabhat Phankong[1], **Kittikorn Meesang**[1], **Sirichai Dangeam**[1], **Surin Ngaemngam**[1], **Promsak Apiratikul**[1], **Prusayon Nintanavongsa**[2], **Saichol Chudjuarjeen**[3], and **Monthon Nawong**[1†], Non-members

ABSTRACT

This paper presents a conceptual design for the cooling system of a 3D oil-immersed distribution transformer operating at 100 kVA/22 kV. The cooling system consists of oil cooling and winding cooling. The heat generated inside the coil and the heat transfer area that connects the coil to the cooling fins of the transformer tank effectively carry heat away from inside the transformer to ensure that its internal temperature does not exceed the designed insulation value. The design boundary conditions also depend on the viscosity of the fluid inside the 3D transformer. The disparities in the average HV winding temperature-rise of 7%, the average LV winding temperature-rise of 4%, and the top oil temperature rise of 16% are all substantial. The results of the calculations align well with the test outcomes, indicating that the methods for building systems to vent oil-intermittent distribution transformers, as outlined in this work, are applicable.

Keywords: Oil-immersed, Transformer temperature, Temperature-rise, Cooling system

Nomenclature:

$\Delta\theta_o$: Top oil temperature-rise
$\Delta\theta_{om}$: Average oil temperature-rise
$\Delta\theta_W$: Average winding temperature-rise
g : Average winding gradient
$\Delta\theta_h$: Hot-spot winding temperature-rise
H : Hot-spot winding
MT_{LV} : Mean turn of low-voltage winding
MT_{LV-HV} : Mean turn of low-voltage and high-voltage winding
MT_{HV} : Mean turn of high-voltage winding
$D2i$: Internal distance of low-voltage coil
$D2o$: Outer distance of low-voltage coil
$D1i$: Internal distance of high-voltage coil
$D1o$: Outer distance of high-voltage coil
CCD : Cooling channel distance
CC : Cooling channel
MID : Main insulation distance
$MISS$: Main insulation strip size
$CMID$: Cooling main insulation distance
CMI : Cooling main insulation
q_1 : Average oil temperature at R_1
q_2 : Average temperature of coil after shutdown
R_1 : Coil resistance measured at constant temperature (q_1)
R_2 : Resistance measured after power supply disconnection
$q_{o(a)}$: Top oil temperature at the end of the test at total losses
$q_{a(a)}$: Average temperature around the transformer at the end of the test at total losses
$q_{o(b)}$: Top oil temperature at the end of the 1-hour test at rated current
$q_{a(b)}$: Average temperature around the transformer at the end of the test at rated current
Dq_o : Oil temperature-rise at the top
$q_{om(a)}$: Average oil temperature at total losses
$q_{om(b)}$: Average temperature of oil at rated current
Dq_{ofm} : Average temperature drop of oil at 1 hour at rated current
Dq_w : Correction of average temperature-rise of coil
g : Difference between the average coil temperature (q_2) and the average oil temperature $q_{om(b)}$ at shutdown
H : Factor S (1.1)
Dq_h : Hot spot winding temperature-rise

1. INTRODUCTION

Power transformers constitute fundamental components of electrical power systems, facilitating the effective distribution and transmission of electricity. The secure, reliable, and economical performance of the system is imperative for the preservation and operation of the entire electrical infrastructure. Temperature monitoring of transformers is of paramount importance, as winding insulation failure can occur in up to 55.6% of instances when the internal temperature surpasses

Manuscript received on August 1, 2025; revised on September 30, 2025; accepted on October 4, 2025. This paper was recommended by Associate Editor Vuttipon Tarateeraseth.

[1]The authors are with Department of Electrical Engineering, Faculty of Engineering, Rajamangala University of Technology Thanyaburi, Pathum Thani, Thailand.

[2]The author is with Department of Computer Engineering, Faculty of Engineering, Rajamangala University of Technology Thanyaburi, Pathum Thani, Thailand.

[3]The author is with Department of Electrical Engineering, Faculty of Engineering, Rajamangala University of Technology Krungthep, Bangkok, Thailand.

[†]Corresponding author: monthon.n@en.rmutt.ac.th

Digital Object Identifier: 10.37936/ecti-eec.2525233.260627

the design insulation limit [1]. The operational lifespan of the transformer insulator will be diminished by 50% under acute loading or transient conditions if the oil temperature exceeds 105˚C.

The internal insulation system and structure of the transformer are safeguarded against overheating through the principles of an efficient cooling system. These mechanisms also contribute to the mitigation of temperatures exceeding the permissible insulation threshold of the transformer. Chen et al. [1] present a cost-effective model to calculate hot spot temperature in three-dimensional (3D) coiled core transformers using top oil temperature. It is accurate but requires empirical validation and refinement for wider use. Li et al. [2] investigate "DC Bias" effects, causing transformer overheating, using temperature-rise tests and simulations needing a 3D update. Limited to a single transformer, more studies are needed for long-term protection. Janic et al. [3] analyze how transformer cooling systems affect efficiency and costs, showing that adjusting cooling fans saves energy and reduces emissions. Results, based on one transformer, could support AI-driven cooling system development, needing wider application studies. Guo et al. [4] employ a 3D model to examine an eco-friendly transformer with an energy-efficient core and vegetable oil. While simulations are promising, real-world validation and studies on the insulation impact of oil are needed. Godec and Kuprešanin [5] critique the IEC 60076-2 standard after two years of testing, noting temperature stabilization weaknesses and proposing improvements; however, broader validation is necessary. Abdali et al. [6] offer a formula for predicting hotspot temperature in transformers, validated with high accuracy but requiring further testing on various models and conditions. Yuan et al. [7] present a dynamic model for temperature changes in dry-type traction transformers on high-speed trains, addressing rapid load shifts from acceleration and braking. Validated with real train data, the model is credible but complex, tailored to a specific transformer model. Future work should extend it to predict insulation lifespan and develop it into a "Digital Twin" for monitoring and maintenance.

Moreover, Rodrigues et al. [8] investigates the placement of sensors in transformers to measure the hottest spot accurately, using 20 fiber optic sensors and CFD simulations. Although validated with real-world data, the study, conducted on a small prototype, may not apply to larger transformers and presents complex, costly installation. The findings aim to guide sensor placement without complex experiments. Msane et al. [9] review 75 papers on IoT technology in transformers, discussing technology, challenges, and future trends like AI and digital twins. The review lacks recent experiments and may soon become outdated amid rapid tech changes. There's a need for accurate IoT-based lifespan prediction models and interoperability standards. Luo et al. [10] describes a system using Fiber Bragg Grating sensors within transformers to measure hot-spot temperature accurately in real time. The system's complex, expensive installation is only suitable at the manufacturing stage. Testing on large transformers is needed to develop predictive service life models. Liu et al. [11] introduces a "quasi-3D" method for quicker, accurate thermal calculations in dry-type transformers, combining 3D and 2D models. It aligns with experimental data but may be less precise in complex areas and needs testing on other transformers under dynamic conditions. Li et al. [12] focuses on the electromagnetic properties of short circuits in three-phase dry-type transformers, particularly winding leakage magnetic fields. Krishman and Nair [13] design transformers for distributed photovoltaic (DPV) generation to meet renewable energy integration needs. Gao et al. [14] enhance understanding of very fast transient overvoltage (VFTO) in transformer windings, crucial for insulation design and protection.

In addition, Sun et al. [15] perform electromagnetic analysis to design cooling structures for 1 MVA HTS power transformers, improving efficiency and compactness. Wu et al. [16] explore flux coupling differential zero-sequence current transformers to advance power system measurement and protection. Accurate heat source calculation is essential for constructing cooling spaces, coils, and fins. This paper presents methods to calculate the heat source temperature of the coil and heat transfer area, considering transformer power at maximum load using empirical methods. According to IEC 60076-2 [17]-[24], top oil and winding temperature-rise will be tested. This paper studies thermal phenomena in a 3D distribution transformer to design a cooling system for a 100 kVA 22 kV/416/240 V 50 Hz Dyn11 ($\pm$2 x 2.5%) transformer, per Technical Specification Division No. RTRN-035/2561. Using the temperature guidelines of IEC 60076-2, it defines the heat dissipation area for the windings. Heat generation is attributed to core and copper losses. The paper uses engineering equations to simulate coil heat production and design a cooling area to transfer heat from the coil to the cooling fins of the tank, maintaining the internal temperature within insulation limits. The concept design determines the space for placing windings according to economic principles and standards.

This paper introduces the conceptual design for the cooling system of the 3D distribution transformer. Section II details the design parameters and fundamental principles. Section III elaborates on the architecture of the transformer cooling system. Section IV discusses the findings from the experiments and simulations.

2. 3D DISTRIBUTION TRANSFORMER

2.1 Components of a 3D Distribution Transformer

Figure 1 illustrates the constituent elements of a 3D distribution transformer, comprising 1) a magnetic core, 2) high-voltage/low-voltage windings, 3) an earthing terminal, 4) a tank and fin, 5) transformer bases, 6) an oil level gauge, 7) a lifting eye, 8) a pressure-relief device, 9) a low-voltage terminal, 10) a high-voltage terminal, 11)

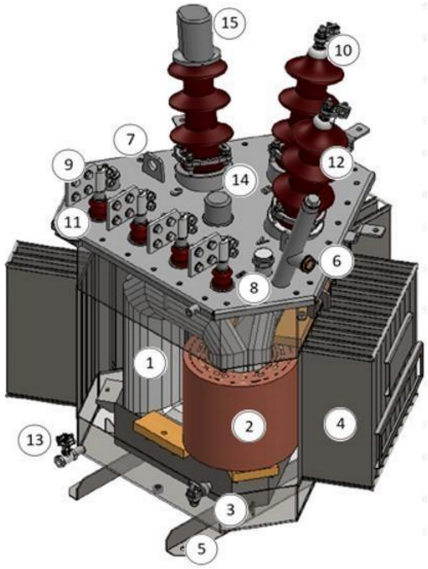

***Fig. 1**: Structure of a 3D distribution transformer.*

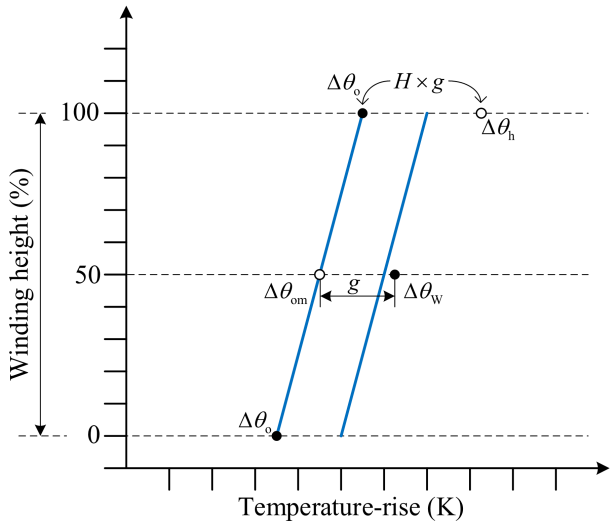

***Fig. 2**: Temperature-rise distribution model for ON cooling methods with the IEC 60076-2 standard.*

a low-voltage bushing, 12) a high-voltage bushing, 13) an oil drain valve, 14) a tap changer, and 15) a bird guard.

The 100 kVA 22 kV/416/240 V 50 Hz Dyn11 (±2 x 2.5%) transformer, operating under ONAN cooling mode and A-class insulation, exhibits no-load losses of 157.1 W and load losses of 1,415.8 W, respectively, and is utilized as a sample transformer for the purpose of designing cooling systems.

2.2 Heat generation in 3D distribution transformer

The generation of heat within the 3D distribution transformer leads to losses, which are primarily categorized into two components: no-load losses and load losses. The predominant source of this thermal energy is the load losses, particularly those arising from copper losses. The heat produced within the transformer

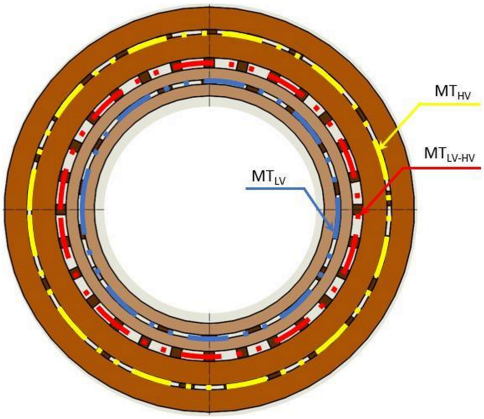

***Fig. 3**: Mean turn of LV windings, LV-HV windings, and HV windings.*

primarily emanates from the low-voltage coil, high-voltage coil, and iron core. It is then transferred to the transformer oil, wherein the accumulated heat elevates to the top of the transformer tank. Conversely, the cooler portion of the oil descends to the bottom of the transformer body, and a fraction traverses through the transformer cooling fins, subsequently being dissipated by the surrounding atmosphere [1].

3. DESIGN OF COOLING SYSTEM FOR 3D DISTRIBUTION TRANSFORMER

3.1 Cooling system

The operational lifespan of transformers may diminish, or they might be susceptible to destruction due to the heat generated during operational processes and inherent internal losses. Therefore, effective heat dissipation is imperative for the optimal functioning of transformers. Transformers that possess superior capabilities for heat dissipation are able to sustain higher loads. In accordance with the principle of thermal conduction, transformer insulation is crucial for facilitating heat transfer from the coils to the exterior. The construction of the cooling system involves the use of oil and winding components. Distribution transformers consist of a core, low-voltage (LV) winding, high-voltage (HV) winding, and primary insulation.

3.2 Relationship of temperature inside transformers

In accordance with the IEC 60076-2 standard [17], the concept of temperature-rise serves as a criterion for determining the design parameters of the internal cooling system of a transformer. This is intended to ensure adherence to the specified temperature-rise limit under a predefined load, thus preventing the surpassing of the operational thermal capacity of the transformer and maintaining a service life consistent with the insulation limitations of the transformer thermal model, as illustrated in Fig. 2. As per the IEC 60076-2 standard, the

***Table 1**: Parameters of the LV side cooling channel.*

Parameter	Value
Main insulation channel distance	20 mm.
Main insulation strip size h	3 mm.
Main insulation strip size b	10 mm.
LV cooling channel distance	20 mm.
LV cooling channel h	4 mm.
LV cooling channel b	10 mm.
LV cooling channel long	215 mm.
Loss of LV 75 °C Pw 275	231.02
LV cooling area	0.252 m^2
MT_{LV}	540.08 mm^2
$MT_{LV\text{-}HV}$	527.83 mm^2
Cooling area inside LV coil	0.104605 m^2
Cooling area LV channel	0.0731 m^2
Cooling area main insulation	0.074175 m^2

***Table 2**: Parameters of the HV side cooling channel.*

Parameter	Value
Main insulation channel distance	15 mm.
Main insulation strip size h	7 mm.
Main insulation strip size b	7 mm.
HV cooling channel distance	20 mm.
HV cooling channel h	4 mm.
HV cooling channel b	10 mm.
HV cooling channel long	215 mm.
Loss of HV 75 °C Pw 275	235.03
HV cooling area	0.345 m^2
MT_{HV}	601.31 mm^2
Cooling area outside HV coil	0.189028 m^2
Cooling area HV channel	0.0817 m^2

principle for calculating the temperature relationship is elucidated. The results will be as delineated in Eqs. (1) and (2):

$$\Delta\theta_{om} = 0.8\Delta\theta_o \tag{1}$$

$$g = \Delta\theta_{om} - \Delta\theta_W \tag{2}$$

According to the IEC 60076-2 standard, it is advised that the$g$value should be set to 15.

3.3 Guidelines for designing cooling systems in high-voltage coils and low-voltage coils

The arrangement of cooling slots within high-voltage and low-voltage coils involves identifying the central circumference of the transformer coil to determine the number of cooling slots, as illustrated in Fig. 3. In the case of LV and HV coils, compressed paper is typically utilized for electrical insulation and cooling purposes. The system is bifurcated into two components: (1) the two types of cooling channels, identified as LV and HV channels, where the number of channels employed is dependent on the cooling area defined by the designer, and (2) the principal insulator, which functions to separate the high-resistance winding from the low-resistance winding, thus reducing potential risks associated with testing and operation. Upon determining the LV cooling area, the surface of the LV coil is defined as the LV cooling area, which then interacts with the oil. This paper evaluates the following three components: (1) LV coil, (2) LV channel, and (3) main insulator. The parameters pertinent to the cooling channels on the LV and HV sides are depicted in Tabs. 1 and 2, respectively, and have been calculated utilizing the designated formulas.

3.3.1 Calculating the mean turn of winding

The mean turn of the LV winding, the mean turn of the LV-HV windings, and the mean turn of the HV winding can be computed in accordance with Eqs. (3)-(5), respectively:

$$MT_{LV} = \left(\frac{D2i - D2o}{2} + D2i\right)\pi \tag{3}$$

$$MT_{LV-HV} = \pi D2o \tag{4}$$

$$MT_{HV} = \left(\frac{(D1i - D1o)}{2} + D1i\right)\pi \tag{5}$$

3.3.2 Calculating the number of cooling channel

The number of LV winding channels, HV winding channels, and main insulators can be determined by Eqs. (6)-(8), respectively.

$$No.\,LV\ winding\ channel = \left(\frac{CCD + CC\,b}{MT_{LV}}\right) - 1 \tag{6}$$

$$No.\,HV\ winding\ channel = \left(\frac{CCD + CC\ b}{MT_{HV}}\right) \tag{7}$$

$$No.\,main\ insulator = \left(\frac{MID + MISS\ b}{MT_{LV-HV}}\right) \tag{8}$$

3.3.3 Calculating the cooling area

The cooling area for the LV channel, the main insulation, and the HV channel can be determined using Eqs. (9)-(13), respectively.

$$\begin{aligned} &Cooling\ area\ inside\ LV\ coil \\ &\quad = (\pi \times D2i \times Winding\ height) \times 10^{-6} \end{aligned} \tag{9}$$

$$\begin{aligned} &Cooling\ area\ LV\ channel \\ &\quad = 2 \times (No.\,LV\ winding\ channel \times CCD \times \\ &\quad\ CC\,h \times Winding\ height) \times 10^{-6} \end{aligned} \tag{10}$$

$$\begin{aligned} &Cooling\ area\ main\ insulation \\ &\quad = (No.\,main\ insulation \times CMID \times \\ &\quad\ CMI\,h \times Winding\ height) \times 10^{-6} \end{aligned} \tag{11}$$

$$\begin{aligned} &Cooling\ area\ HV\ channel \\ &\quad = 2 \times (No.\,HV\ winding\ channel \times CCD \times \\ &\quad\ CC\,h \times Winding\ height) \times 10^{-6} \end{aligned} \tag{12}$$

$$\begin{aligned} &Cooling\ area\ outside\ HV\ coil \\ &\quad = (\pi \times D1o \times Winding\ height) \times 10^{-6} \end{aligned} \tag{13}$$

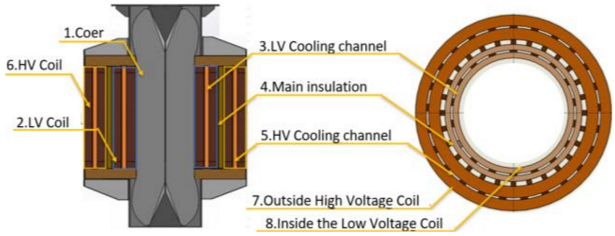

***Fig. 4**: Cooling structure in coils.*

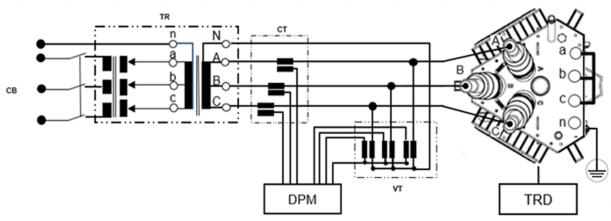

***Fig. 5**: Short-circuit test for temperature-rise.*

3.3.4 Calculating the gradient

The gradient values for the LV and HV coils can be computed based on the watts per cooling area as delineated in Eqs. (14) and (15), respectively.

$$LV\ Gradient = \left(0.0147 \times \frac{LV\ Watt}{Cooling\ Area}\right) + 5.8235 \tag{14}$$

$$HV\ Gradient = \left(0.0147 \times \frac{HV\ Watt}{Cooling\ Area}\right) + 5.8235 \tag{15}$$

3.3.5 Calculating the average oil temperature

The computation of the average oil temperature is derived from the maximal gradient value, which is quantified in degrees Celsius, as detailed in Eq. (16).

$$Average\ oil\ temp = Top\ oil\ design - Max.\ gradient \tag{16}$$

Consequently, the top oil temperature is determinable utilizing Eq. (17).

$$Top\ oil\ temp = \frac{Average\ oil\ temp}{0.8} \tag{17}$$

3.3.6 Calculating the temperature-rise

The temperature-rise for the LV and HV coils is determined by employing Eqs. (18) and (19), respectively.

$$LV\ temp\ rise = Top\ oil\ temp + LV\ gradient \tag{18}$$

$$HV\ temp\ rise = Top\ oil\ temp + HV\ gradient \tag{19}$$

As a result, the cooling structure for the transformer coils will be implemented using the cooling channel shown in Fig. 4.

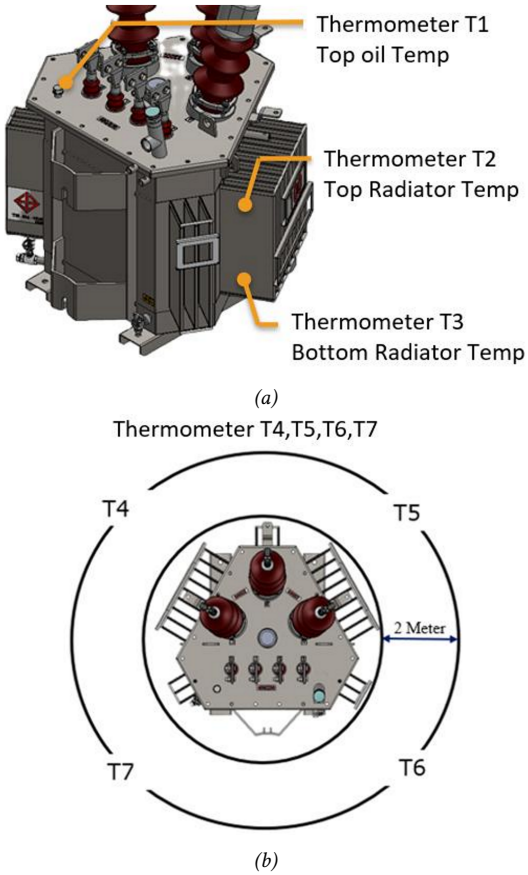

***Fig. 6**: Installation location of temperature sensor in temperature-rise test. (a) transformer temperature measurement (b) ambient temperature measurement.*

4. EXPERIMENTAL SETUP

4.1 Temperature-rise test of transformer

The objective of this test is to ascertain the temperature-rise of the top oil, the average temperature-rise of the transformer windings, and the temperature-rise at the hot spot of the windings under steady-state conditions while the transformer operates at maximum load. The thermal output resulting from all losses must remain within the defined standard. Failure to meet the standard criteria indicates the transformer is either underrated or operating below its full kilovolt-ampere (kVA) capacity.

The principle and methodology for measuring temperature rise may be executed via a short-circuit test, employing the total loss value obtained by calculating the load loss at a reference temperature of 75˚C, along with the no-load loss value.

The methodology for the testing procedure is delineated in the subsequent sections:

1. Enter the total loss value and proceed with testing until the rate of change in the top oil temperature rise stabilizes, that is, when the fluctuation in the rate of top oil temperature-rise or fall does not exceed 1˚C per hour for three consecutive hours. Moreover, employ the average value recorded during the final hour of

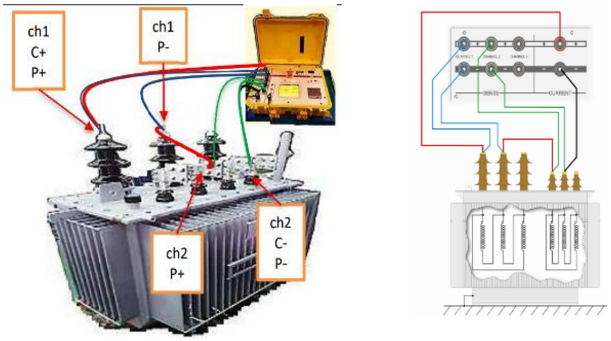

***Fig. 7**: Circuit for measuring winding resistance.*

***Table 3**: Results of temperature-rise from design guidelines.*

Parameter	Designed value (K)
Top oil temperature $\Delta\theta_o$	44
LV temperature-rise $\Delta\theta_{wLV}$	55
HV temperature-rise $\Delta\theta_{wHV}$	53.2

testing as the experimental finding for determining the top oil temperature-rise, as illustrated in Fig. 5. The testing apparatus included 1) a 100 A circuit breaker (CB), 2) a step-down transformer (TR), 3) a current transformer (CT), 4) a voltage transformer (VT), 5) a digital power meter (DPM), and 6) a temperature recorder (TRD).

2. Enter the rated current for the tap under examination. Upon acquiring the test results concerning the elevation in the upper oil temperature, reduce the voltage to the rated current for a duration of one hour. During this period, record the top oil temperature, top radiator temperature, bottom radiator temperature, and ambient temperature at 5-minute intervals. Figure 6 illustrates the installation location of the temperature sensor utilized in the temperature rise test.

4.2 Winding resistance value

Upon completion of the initial step, it is imperative that the power supply and short-circuit connections be disengaged within one hour. The resistance value of the coils must be measured promptly and expeditiously. The resistance values for both the high-voltage and low-voltage coils must be recorded within two minutes. Subsequent measurements of the resistance value are to be conducted after a lapse of 20 minutes from the initial disconnection of the power supply. Figure 7 illustrates the method for measuring winding resistance using a megaohmmeter.

The plotted resistance values are extrapolated backward on a curve to determine the outside-channel resistance value (R_2), with the tested values subsequently being entered into Eqs. (20)-(27).

$$Dq_o = q_{o(a)} - q_{a(a)} \tag{20}$$

$$q_{om(a)} = Dq_o \times 0.8\% \tag{21}$$

$$q_{om(b)} = (q_{o(b)} \times q_{a(b)}) \times 0.8\% \tag{22}$$

$$q_2 = \frac{R_1}{R_2}(235 \times \theta_1) - 235 \tag{23}$$

$$Dq_{ofm} = q_{om(a)} - q_{om(b)} \tag{24}$$

$$Dq_w = q_2 + (Dq_{ofm} - q_{a(a)}) \tag{25}$$

$$q = (q_2 - q_{om(b)}) \tag{26}$$

$$Dq_h = q_{om(a)} - q_{om(b)} \tag{27}$$

The test requirements according to IEC 60076-2 Edit 3.0 -2011-02, Power transformer, Part 2: Temperature-rise for liquid-immersed transformers, stipulate the following practices:The temperature during the test shall be in the range of 10 - 40°C, and the humidity during the test shall not exceed 90%. Before testing, the tested transformer shall be placed in the test room environment for at least 3 hours. The transformer must be placed in the test room environment to avoid errors in measurement and test value processing.

5. RESULTS AND DISCUSSION

5.1 Results from design guidelines

Based on the parameters of the LV side cooling channel and those of the HV side cooling channel, as presented in Tabs. 1 and 2, respectively, the average oil temperature, top oil temperature, and temperature-rise for both LV and HV sides can be computed utilizing the IEC 60076-2 standard in accordance with the parameters of the 3D distribution transformer, as depicted in Tab. 3.

5.2 Experimental results

The short-circuit method is employed to perform temperature-rise tests, as illustrated in Fig. 5. The procedure will be executed considering total losses, load losses at 75°C, and no-load losses. These constitute the stages of testing. The transformer testing temperature is monitored using thermometers, which are installed and illustrated in Fig. 6. The temperature-rise of the distribution transformer during testing is presented in Tab. 4. Testing will continue until the rate of increase in the top oil temperature remains steady, meaning until the top oil temperature varies at a rate that does not exceed 1°C per hour for a period of three consecutive hours. The increase in temperature of the top oil will be assessed during the final hours of testing, during which the average data will be applied.

Upon obtaining the results pertaining to the elevated top oil temperature test, it is advisable to reduce the voltage to the rated current for a period of one hour. It is imperative to monitor and document the top oil temperature, the temperature at the upper radiator, the

***Table 4**: Oil temperature change rate test results for 3-phase transformer 100 kVA 22kV 416/240V 50Hz Dyn11 (±2×2.5%).*

Time	Tested			Top oil Temp. (°C)	Radiator Temp. (°C)		Ambient Temp. (°C)					Top oil Temp. Rise (K)
	Voltage (V)	Current (A)	Power (W)		Top	Bottom						
				T1	T2	T3	T4	T5	T6	T7	AVG	
18:00	1011.0	2.965	1573	31.5	31.2	31.0	31.3	31.2	31.1	31.3	31.2	0.3
19:00	980.9	2.858	1578	41.9	41.2	35.7	31.2	31.1	30.9	31.0	31.1	10.9
20:00	972.7	2.821	1581	51.3	50.1	41.4	31.1	30.0	30.8	30.9	31.0	20.4
21:00	963.6	2.793	1577	57.4	56.1	45.3	31.0	30.9	30.7	30.8	30.9	26.6
22:00	961.5	2.783	1580	61.4	60.0	47.9	31.0	30.8	30.6	30.7	30.8	30.6
23:00	958.3	2.771	1579	64.0	62.6	49.3	30.8	30.7	30.3	30.6	30.6	33.4
0:00	954.0	2.749	1569	65.4	64.1	50.2	30.7	30.6	30.2	30.5	30.5	34.9
1:00	950.8	2.753	1568	66.1	64.8	50.4	30.5	30.1	29.7	30.0	30.1	36.0
2:00	956.6	2.751	1565	66.4	65.2	50.5	29.9	29.8	29.5	29.8	29.8	36.7
3:00	954.6	2.763	1577	66.5	65.2	50.4	29.5	29.6	29.2	29.6	29.5	37.0
4:00	960.4	2.757	1570	66.2	65.2	50.2	29.3	29.3	29.0	29.3	29.2	37.2
5:00	956.8	2.790	1589	65.9	64.9	49.8	29.0	29.0	28.7	29.0	28.9	37.3
6:00	957.7	2.764	1577	65.8	64.6	49.6	28.8	28.8	28.5	28.8	28.7	37.2
7:00	909.8	2.766	1579	65.8	64.6	49.6	28.8	28.8	28.5	28.8	28.7	37.1
8:00	909.2	2.626	1421	65.8	64.6	49.7	28.8	28.8	28.5	28.8	28.7	37.1

***Table 5**: Temperature test results at the end of the run with total loss injection.*

Parameter	Value
Top- liquid temperature $\theta_{o(a)}$	65.1°C
Ambient temperature at hot state $\theta_{amb(a)}$	28.9°C

***Table 6**: Test result calculation of top liquid temperature rise and average liquid temperature.*

Parameter	Value
Top- liquid temperature rise $\Delta\theta_o = \Delta_o - \theta_{amb(a)}$	37.1K
Average liquid temperature (a) $\theta_{amb(a)} = \Delta\theta_0 \times 80\%$	29.7°C

temperature at the lower radiator, and other values recorded during the rated current input interval every hour. Table 4 presents the recorded values of top oil temperature, HV winding temperature, and LV winding temperature. The testing indicates that the mean temperature of both windings complies with the standard limits at 08:00.

Subsequently, the oil temperature values presented in Tab. 4 and the transformer winding resistance values depicted in Fig. 8 are computed to ascertain the values illustrated in Tabs. 5-9, which correspond to Eqs. (20)-(27). These computations ultimately yield the temperature-rise calculation results, as demonstrated in Tab. 10.

The temperature test results under full load conditions are conducted in accordance with the IEC 60076-2 standard. The design specifications for internal heat generation adhere to Technical Specification Division No. RTRN-035/2018, stipulating the ambient temperature of 50˚C, top oil temperature-rise of 50˚C, coil temperature-rise of 55˚C, and total losses of 1547 W. Upon comparing

***Table 7**: Test result calculation of top liquid temperature rise and average liquid temperature.*

Parameter	Value
Top-liquid temperature during the 1h test $\theta_{(b)}$	65.1°C
Ambient temperature at hot state $\theta_{amb(b)}$	28.9°C
Average liquid temperature (b) $\theta_{om(b)} = \theta_{(b)} - \theta_{amb(b)} \times 80\%$	29.0°C
Fall of Average liquid temperature $\Delta\theta_{ofm} = \theta_{om(a)} - \theta_{om(b)}$	0.7K

***Table 8**: Test result average temperature of the winding at the instant of shutdown.*

Parameter	Value
High voltage winding θ_{2HV}	80.2°C
Low voltage winding θ_{2LV}	76.9°C

***Table 9**: Correction of the winding average temperature-rise of the winding test result.*

Parameter	Value
High voltage winding $\Delta\theta_{wHV} = \theta_{2HV} + \Delta\theta_{ofm} - \theta_{amb(a)}$	53.0K
Low voltage winding $\Delta\theta_{wLV} = \theta_{2LV} + \Delta\theta_{ofm} - \theta_{amb(a)}$	49.6K

the temperature-rise test results with the coil cooling system design, it was determined that the results yielded a heat value for the upper oil. According to the design specifications, the heat value of the high voltage coil differed by 16%. Similarly, the heat value of the HV winding deviated by 4% from the design, while the heat

***Table 10**: Temperature-rise test results.*

Parameter	Measured value (K)
Top oil temperature rise $\Delta\theta_o$	37.1
LV winding temperature rise $\Delta\theta_{wLV}$	54.2
HV winding temperature rise $\Delta\theta_{wHV}$	52.1

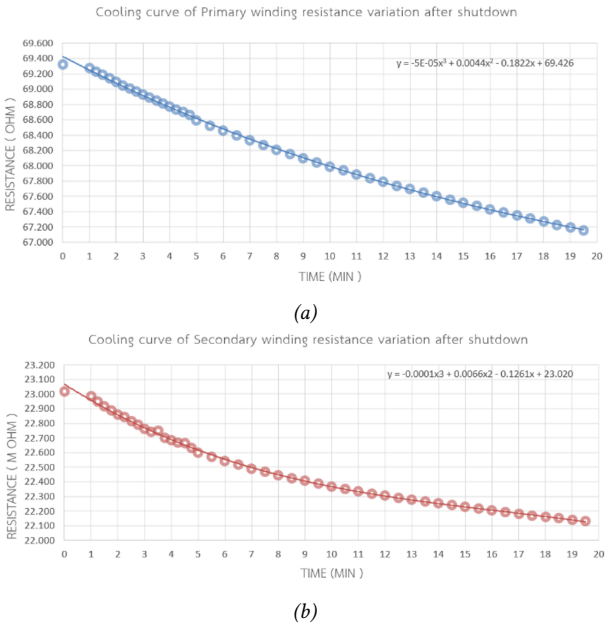

***Fig. 8**: Graph results of the winding resistance test after shutdown. (a) Primary winding (b) Secondary winding.*

value of the LV winding exhibited a 7% difference from the design.

6. CONCLUSION

This paper examines the temperature distribution within a 3D oil-immersed transformer with a capacity of 100 kVA/22 kV. The calculated percentages are as follows: the increase in the top oil temperature is 16%, the average temperature rise of the high-voltage winding is 7%, and the average temperature rise of the low-voltage winding is 4%. The outcomes of the calculations closely align with experimental results, thereby substantiating the applicability of the methodologies employed for designing venting systems for oil-immersed distribution transformers as delineated in this research. The computational model consistently determines the temperature distribution within the windings of the 3D distribution transformer under full load current conditions, given ambient temperatures do not surpass 55°C.

ACKNOWLEDGEMENT

A preliminary version of this work has been published in ECTI-CON 2024 [25]. This research was supported by Precision Electric Manufacturing Co., Ltd.

REFERENCES

[1] Q. Chen, S. Chen, W. Huang, W. Zhang, and K. Li, "Research on Inversion Model of Winding Hot Spot Temperature of 10-kV Oil-Immersed Three-Dimensional Coiled Core Transformer," *IEEE Access*, vol. 12, pp. 97691–97700, 2024.

[2] M. Li, Z. Wang, J. Zhang, Z. Ni, and R. Tan, "Temperature Rise Test and Thermal-Fluid Coupling Simulation of an Oil-Immersed Autotransformer Under DC Bias," *IEEE Access*, vol. 9, pp. 32835–32844, 2021.

[3] Z. Janic, N. Gavrilov, and I. Roketinec, "Influence of Cooling Management to Transformer Efficiency and Ageing," *Energies*, vol. 16, no. 12, Jun. 2023.

[4] J. Guo, K. Fan, B. Yang, H. Yang, Q. Peng, and H. Zheng, "Investigation on Temperature Rise Characteristic and Load Capacity of Amorphous Alloy Vegetable Oil Distribution Transformers with 3D Coupled-Field Method," *Machines*, vol. 10, no. 1, Jan. 2022.

[5] Z. Godec and V. Kuprešanin, "Temperature rise of power transformers: comments and proposals to IEC 60076-2:2011," *Journal of Energy - Energija*, vol. 63, no. 1–4, pp. 22-34, Jul. 2022.

[6] A. Abdali, A. Abedi, K. Mazlumi, A. Rabiee, and J. M. Guerrero, "Novel Hotspot Temperature Prediction of Oil-Immersed Distribution Transformers: An Experimental Case Study," in *IEEE Transactions on Industrial Electronics*, vol. 70, no. 7, pp. 7310-7322, Jul. 2023.

[7] S. Yuan, M. Wang, Z. Zhou, C. Liang, X. Wang, and Z. Li, "Dynamic Temperature Distribution Modeling Method of Dry-Type On-Board Traction Transformer in EMU," in *IEEE Transactions on Instrumentation and Measurement*, vol. 74, pp. 1-12, 2025.

[8] T. F. Rodrigues *et al.*, "Evaluation of Power Transformer Thermal Performance and Optical Sensor Positioning Using CFD Simulations and Temperature Rise Test," in *IEEE Transactions on Instrumentation and Measurement*, vol. 72, pp. 1-11, 2023,

[9] M. R. Msane, B. Thango, and K. A. Ogudo, "Condition Monitoring of Electrical Transformers Using the Internet of Things: A Systematic Literature Review," *Applied Sciences*, vol. 14, no. 21, pp. 9690–9690, Oct. 2024

[10] C. Luo, Z. Li, B. Yang, Z. Zhao and C. Li, "Hot-Spot Dynamic Temperature Rise of Oil-Immersed Transformer Through FBG-Based Multipoint Sensing System," in *IEEE Sensors Journal*, vol. 25, no. 13, pp. 25743-25753, Jul. 2025.

[11] C. Liu, J. Ruan, W. Wen, R. Gong, and C. Liao, "Temperature rise of a dry-type transformer with quasi-3D coupled-field method," *IET Electric Power Applications*, vol. 10, no. 7, pp. 598–603, Apr. 2016.

[12] Y. Li, J. Du, Y. Jing, and D. Zou, "Simulated Analysis and Experimental Study of Winding Leakage

Magnetic Field in Short Circuit of Three-Phase Three-Column Dry-Type Transformer," in *2020 IEEE International Conference on Applied Superconductivity and Electromagnetic Devices (ASEMD)*, Tianjin, China: IEEE, Oct. 2020, pp. 1–2.

[13] R. Krishnan and K. R. M. Nair, "Transformer for Distributed Photovoltaic (DPV) Generation," *2018 International Conference on Electrical, Electronics, Communication, Computer, and Optimization Techniques (ICEECCOT)*, Msyuru, India, 2018, pp. 1659-1663.

[14] Y. Gao, Y. Li, C. Ding, and G. Wang, "Computation of very fast transient over-voltages (VFTO) in transformer windings," in *2009 International Conference on Electrical Machines and Systems*, Tokyo, Japan: IEEE, Nov. 2009, pp. 1–4.

[15] R. M. Sun, J. X. Jin, X. Y. Chen, C. L. Tang, and Y. P. Zhu, "Critical Current and Cooling Favored Structure Design and Electromagnetic Analysis of 1 MVA HTS Power Transformer," *IEEE Trans. Appl. Supercond.*, vol. 24, no. 5, Oct. 2014.

[16] W. Wu, K. Hou, D. Wu, K. Wu, and B. Liu, "Optimal Design of Flux Coupling Differential Zero-Sequence Current Transformer," in *2020 4th International Conference on Power and Energy Engineering (ICPEE)*, Xiamen, China: IEEE, Nov. 2020, pp. 157–162.

[17] International Electrotechnical Commission, *Power transformers. Part 2: temperature rise for liquid-immersed transformers = Transformateurs de puissance. Partie 2 : echauffement des transformateurs immergés dans le liquide.* Genove: International Electrotechnical Commission, 2011.

[18] E. I. Amoiralis, M. A. Tsili, A. G. Kladas, and A. T. Souflaris, "Distribution transformer cooling system improvement by innovative tank panel geometries," *IEEE Trans. Dielect. Electr. Insul.*, vol. 19, no. 3, Jun. 2012.

[19] K. S. Kassi, I. Fofana, M. I. Farinas, and C. Volat, "Studying power transformers cooling effectiveness from computational fluid dynamics approach," in *2016 IEEE Electrical Insulation Conference (EIC)*, Montreal, QC, Canada: IEEE, Jun. 2016, pp. 13–16.

[20] M. Taghilou, M. Mirsalim, M. Eslamian, and A. Teymouri, "Comparative Study of Shield Placement to Mitigate the Stray Loss of Power Transformers Based on 3D-FEM Simulation," in *2023 3rd International Conference on Electrical Machines and Drives (ICEMD)*, Tehran, Iran, Islamic Republic of: IEEE, Dec. 2023, pp. 1–7.

[21] L. Raeisian, H. Niazmand, E. Ebrahimnia-Bajestan, and P. Werle, "Thermal management of a distribution transformer: An optimization study of the cooling system using CFD and response surface methodology," *International Journal of Electrical Power & Energy Systems*, vol. 104, pp. 443–455, Jan. 2019.

[22] Z. Kou and J. Zhao, "Three-dimensional Structure Simulation of Strong Oil Air-cooled Transformer and Finite Element Analysis of Internal Temperature Fluid Field," in *2019 IEEE 3rd Conference on Energy Internet and Energy System Integration (EI2)*, Changsha, China: IEEE, Nov. 2019, pp. 273–278.

[23] Y. Wu, L. Liu, C. Shi, K. Ma, Y. Li, and H. Mu, "Research on Measurement Technology of Transformer No-load Loss Based on Internet of Things," in *2019 IEEE 8th International Conference on Advanced Power System Automation and Protection (APAP)*, Xi'an, China: IEEE, Oct. 2019, pp. 150–153.

[24] V. Shiravand, J. Faiz, M. H. Samimi, and M. Mehrabi-Kermani, "Prediction of transformer fault in cooling system using combining advanced thermal model and thermography," *IET Generation Trans & Dist*, vol. 15, no. 13, Art. no. 13, Jul. 2021.

[25] K. Meesang, N. Phankong, P. Apiratikul, M. Nawong, S. Dangeam, and W. Yuakthong, "Design of 3D-Cooling System of 100 kVA/22 kV Distribution Transformer," in *2024 21st International Conference on Electrical Engineering/Electronics, Computer, Telecommunications and Information Technology (ECTI-CON)*, Khon Kaen, Thailand: IEEE, May 2024, pp. 1–4.

Nathabhat Phankong received the B.Eng. (Hons.) degree and M.Eng. degree in electrical engineering from King Mongkut's University of Technology Thonburi (KMUTT), Bangkok, Thailand in 1999 and 2003, respectively, and the Ph.D. degree in electrical engineering from Kyoto University, Japan in 2010. He is currently an Associate Professor with the Department of Electrical Engineering, Rajamangala University of Technology Thanyaburi, Pathum Thani, Thailand. His research interests are mainly in power electronic systems and conversion.

Kittikorn Meesang received his B.Eng. degree in electrical engineering from Pathum thani University, Pathum Thani, Thailand, in 2010, M.Eng. degree in electrical engineering from Rajamangala University of Technology Thanyaburi, Pathum Thani, Thailand, in 2025. Currently, he is engineer in Precise Electric Manufacturing Co., Ltd. His research interests are primarily focused on power systems.

Sirichai Dangeam received his B.Eng. degree in electrical engineering from Rajamangala University of Technology Thanyaburi, Pathumtani, Thailand, in 1995, M.Eng. degree in electrical engineering from King Mongkut's University of Technology North Bangkok, Bangkok, Thailand, in 2003, and D.Eng. degree in electrical engineering at the King Mongkut's Institute of Technology Ladkrabang, Bangkok, Thailand. He is currently working as an associate professor at the Department of Electrical Engineering, Faculty of Engineering, Rajamangala University of Technology Thanyaburi, Pathum Thani,

Thailand. His main research interests include power converters and electric drives.

Surin Ngaemngam received his Ph.D. degree in Energy Science from Kyoto University, Japan. He is currently a lecturer and researcher at the Faculty of Engineering, Rajamangala University of Technology Thanyaburi, Thailand. His research interests include smart metering systems, IoT-based automation, mathematical modeling, and energy monitoring technologies.

Promsak Apiratikul received his B. Eng. and M. Eng. degrees in Electrical Eng. from Rajamangala University of Technology Thanyaburi, King Mongkut's Institute of Technology Ladkrabang, and M. Eng. (Safety Eng.), Kasetsart University (KU) Bangkok, Thailand, in March 1999, September 2002 and June 2003, respectively. He has worked as lecturer at the Department of Electrical Power Engineering of RMUTT since November 1999. he worked as research associate at High Voltage Laboratory, RMUTT. He is currently a doctoral student at the Kasetsart University, Thailand. His main research interests are applications of High Voltage Technology, Partial Discharge Analysis, Ozone Generator and Electrical Safety Engineering System.

Prusayon Nintanavongsa (SM'24) received the B.E. degree in electrical engineering from SIIT, Bangkok, Thailand, in 1999, the M.E. degree in computer engineering from KMUTT, Bangkok, in 2001, the M.S. degree in electrical engineering from Boston University, Boston, MA, USA, in 2006, and the Ph.D. degree in computer engineering from Northeastern University, Boston, MA, USA, in 2013., Currently, he is an associate professor in the Computer Engineering Department at Rajamangala University of Technology Thanyaburi, Thailand. His expertise and research interests lie in RF energy harvesting circuit design, protocol design in energy harvesting wireless sensor networks, and ultra-low power wireless sensor networks. ,Dr. Nintanavongsa won a best paper award at the IEEE ICNC conference in 2013. He was a recipient of the Royal Thai government scholarship.

Saichol Chudjuarjeen received the B.Eng. degree from the Mahanakorn University of Technology, Thailand, in 2000, the M.Eng. degree and the Ph.D. degree in electrical and computer engineering from King Mongkut's University of Technology Thonburi, Bangkok, Thailand in 2005 and 2011, respectively. He is an Associate Professor with the Department of Electrical Engineering, Rajamangala University of Technology Krungthep, Bangkok, Thailand. His research interests include high-frequency resonant inverters for induction heating, current-source and voltage-source inverters, Renewal Energy, Green Environment, Wireless Technology and control of power-electronic systems.

Monthon Nawong received the M.Eng. degrees in Control Engineering and D.Eng. degrees in Electrical Engineering from King Mongkut's Institute of Technology Ladkrabang, Bangkok, Thailand, in 2003 and 2014, respectively. Currently, he is an assistance professor in Department of electrical engineering, Faculty of Engineering, Rajamangala University of Technology Thanyaburi, Thailand. His main research interests include applications of Power Electronics.